

Evolution of regulatory networks towards adaptability and stability in a changing environment

Deok-Sun Lee^{1,*}

¹*Department of Physics, Inha University, Incheon 402-751, Korea*

(Dated: November 26, 2014)

Diverse biological networks exhibit universal features distinguished from those of random networks, calling much attention to their origins and implications. Here we propose a minimal evolution model of Boolean regulatory networks, which evolve by selectively rewiring links towards enhancing adaptability to a changing environment and stability against dynamical perturbations. We find that sparse and heterogeneous connectivity patterns emerge, which show qualitative agreement with real transcriptional regulatory networks and metabolic networks. The characteristic scaling behavior of stability reflects the balance between robustness and flexibility. The scaling of fluctuation in the perturbation spread shows a dynamic crossover, which is analyzed by investigating separately the stochasticity of internal dynamics and the network structures different depending on the evolution pathways. Our study delineates how the ambivalent pressure of evolution shapes biological networks, which can be helpful for studying general complex systems interacting with environments.

PACS numbers: 89.75.Hc, 87.23.Kg, 05.65.+b, 87.16.Yc

I. INTRODUCTION

The global organization of complex molecular interactions within and across cells is being disclosed by the graph-theoretic approaches [1–4]. The obtained cellular networks exhibit universal topological features which are rarely found in random networks, such as broad degree distributions [5] and high modularity [6]. Their origins and implications to cellular and larger-scale functions have thus been of great interest. Diverse network models based on simple mechanisms of adding and removing nodes and links have been proposed [7–9]. Those models capture the common aspects, like the preferential attachment [10], of biological processes such as the duplication, divergence, and recruitment of genes, proteins, and enzymes, and successfully reproduce the empirical features of biological networks, suggesting that the former can be the origin of the latter. Yet it remains to be explored what drives such construction and remodeling of biological networks functioning in living organisms. A population of living organisms find the typical architecture and function of their cellular networks changing with time. Such changes on long time scales are made by the organisms of different traits, giving birth to their descendants with different chances, that is, by evolution [11, 12]. Therefore, it is desirable to investigate how the generic features of evolution lead to the emergence of the common features of biological networks.

Living organisms are required to possess adaptability and stability simultaneously [13]. To survive and give birth to descendants in fluctuating environments, the ability to adjust to a changed environment is essential [14], which leads to, e.g., phenotypic diversity and the advantage of bet-hedging strategy [14]. At the same

time, the ability to maintain the constant structure and perform routine important functions regularly, such as cell division and heat beats, is highly demanded. Therefore, in a given population, the cellular networks supporting higher adaptability and stability are more likely to be inherited, which leads the representative topology and function of the cellular networks to evolve over generations.

Here we study how such evolutionary pressure shapes the biological networks. We propose a network model, in which links are rewired such that both adaptability and stability are enhanced. The dynamics of the network is simply represented by the Boolean variables assigned to each node regulating one another [15]. The Boolean networks have been instrumental for studying the gene transcriptional regulatory networks [16] and the metabolic networks [17]. This model network is supposed to represent the network structure typical of a population. The evolution of Boolean networks towards enhancing adaptability [18–22], stability [23–31], or both [32] has been studied, mostly by applying the genetic algorithm or similar ones to a group of small networks. In particular, the model networks which evolve by rewiring links towards local dynamics being neither active nor inactive have been shown to reproduce the critical global connectivity and many of the universal features of real-world biological networks [33–36], demonstrating the close relation between evolution and the structure of biological networks. However, the evolutionary evaluation and selection are made for each whole organism, not for part of it. In the simulated evolution of our model, the adaptability and the stability of the *global* dynamical state are evaluated in the wild-type network and its mutant network, differing by a single link from each other, and the winner of the two becomes the wild-type in the next step. The study of this model leads us to find that sparse and heterogeneous connectivity patterns emerge, which are consistent with the gene transcriptional regulatory net-

* deoksun.lee@inha.ac.kr

works and the metabolic networks of diverse species. The scaling behavior of stability with respect to system size suggests that the evolved networks are critical, lying at the boundary between the inflexible ordered phase and the unstable chaotic phase.

Our study also shows how the nature of fluctuations and correlations changes by evolution. The extent of perturbation spread characterizing the system's stability fluctuates over different realizations of evolution. The fluctuation turns out to scale linearly with the mean in the stationary state of evolution while the square-root scaling holds in the transient period. We argue that this dynamic crossover is rooted in the variation of the combinatorial impacts of the structural fluctuation, driven by evolution, and the internal stochasticity. The scaling of the correlation volume, representing the typical number of nodes correlated with a node, is another feature of the evolved networks. Our results thus show the universal impacts of biological evolution on the structure and function of biological networks and illuminate the nature of correlations and fluctuations in such evolving systems distinguished from randomly-constructed or other artificial systems.

The paper is organized as follows. The network evolution model is described in detail in Sec. II. The emergent structural and functional features are presented in Sec. III. In Sec. IV, we represent the Hamiltonian approach to a generalized model, including our model in a limit, and show the robustness of the obtained results. The scaling behaviors of the fluctuation of perturbation spread and the correlation volume are analyzed in Secs. V and VI, respectively. We summarize and discuss the results of our study in Sec. VII.

II. MODEL

We consider a network in which the node activities are regulated by one another. The network may represent the transcriptional regulatory network of genes, in which the transcription of a gene is affected by the transcriptional factors encoded from other genes, or the metabolic network of metabolites and reactions, the concentrations and fluxes of which are correlated. Various cellular functions are based on those elementary regulations. The model network does not mean that of a specific organism but is representative of the cellular networks of a population of organisms, which evolve with time. In our model the network evolution is made by adding or removing links, representing the establishment of new regulatory inputs or the loss of existing targets possibly caused by point mutations in the regulatory or coding regions of DNA [16, 32].

To be specific, we consider a network G of N nodes which are assigned Boolean variables $b_i = \pm 1$ for $i = 1, 2, \dots, N$. b_i represents whether a node i is active or inactive in terms of the transcription of the messenger RNA, the flux of the corresponding chemical reaction, or

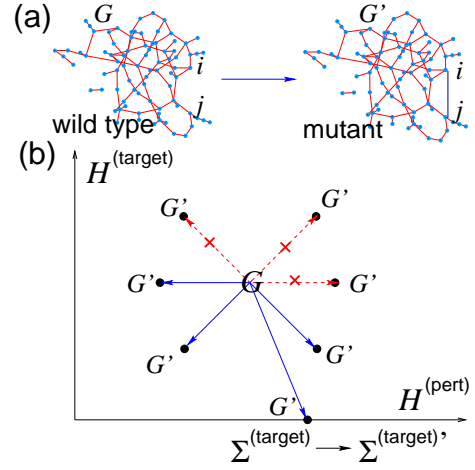


FIG. 1. (Color online) Evolving network model. (a) A mutant G' is generated by adding or removing a link randomly in the wild-type G , here between nodes i and j . (b) The transition from G to G' happens if $H_{G'}^{(target)} < H_G^{(target)}$ or if $H_{G'}^{(pert)} < H_G^{(pert)}$ and $H_{G'}^{(target)} = H_G^{(target)}$. A new target state $\Sigma^{(target)'}$ is generated if $H_{G',t}^{(target)} = 0$.

the concentration of the metabolite. The global dynamical state is represented by $\Sigma = \{b_1, b_2, \dots, b_N\}$. Initially L_0 directed links are randomly wired and b_i 's are set to 1 or -1 randomly. A link from node j to node i , with the adjacency matrix $A_{ij} = 1$, indicates the regulation of the activity of i by j [16, 17]. $b_i(\tau + 1)$ of node i at the microscopic time step $\tau + 1$ is determined by its regulators at τ as

$$b_i(\tau + 1) = F_i(\{b_j(\tau) | A_{ij} = 1\}), \quad (1)$$

where F_i is the time-constant regulation function for node i , taking a value 1 or -1 for each of all the 2^{k_i} states of k_i regulators with $k_i = \sum_j A_{ij}$. A target state $\Sigma^{(target)} = \{b_1^{(target)}, b_2^{(target)}, \dots, b_N^{(target)}\}$ is demanded of the network by the environment and the distance between Σ and $\Sigma^{(target)}$ quantifies the adaptation to the environment.

The dynamical state $\Sigma(\tau) = \{b_1(\tau), b_2(\tau), \dots, b_N(\tau)\}$ is updated every microscopic time step τ as in Eq. (1). Also the structure of the network G , including its adjacency matrix A and the regulating functions $\{F\}$, evolves on a longer time scale as follows. At $\tau = t\tau_m$ with $t = 0, 1, 2, \dots$ the macroscopic time step and τ_m a time constant, a mutant network G' is generated, which is identical to the wild-type G except that it has one more or less link with a different regulation function (See Fig. 1). Then we let the dynamical state $\Sigma(\tau)$ evolve on G and G' , respectively, for $t\tau_m \leq \tau < (t+1)\tau_m$. Due to their structural difference, the $\Sigma(\tau)$'s may evolve differently although they are set equal initially at $\tau = t\tau_m$. At $\tau = (t+1)\tau_m$, the adaptability and the stability of the time trajectories $\{\Sigma(\tau) | t\tau_m \leq \tau < (t+1)\tau_m\}$ on G

and G' are evaluated in terms of the Hamming distances, $H_{G,t}^{(\text{target})}$, $H_{G',t}^{(\text{target})}$, $H_{G,t}^{(\text{pert})}$, and $H_{G',t}^{(\text{pert})}$, where the first two characterize the adaptation to the environment and the latter two represent the typical extent of perturbation spread. The winner of G and G' is determined in the way detailed below, which then becomes the wild-type G for $(t+1)\tau_m \leq \tau < (t+2)\tau_m$ competing with its mutant. These procedures are repeated for $t = 0, 1, 2, \dots$

The adaptability of a Boolean network G at time t is here quantified by the average Hamming distance between $\Sigma(\tau)$ and a given target state $\Sigma^{(\text{target})}$ [18–22] over a microscopic time interval as

$$H_{G,t}^{(\text{target})} = \frac{1}{\tau_m - \tau_s} \sum_{\tau=t\tau_m+\tau_s}^{(t+1)\tau_m} H(\Sigma(\tau), \Sigma^{(\text{target})}),$$

$$H(\Sigma, \Sigma^{(\text{target})}) = \frac{1}{N} \sum_{i=1}^N \left(1 - \delta_{b_i, b_i^{(\text{target})}}\right) \quad (2)$$

where $\delta_{a,b}$ is the Kronecker delta function. τ_s is a microscopic-time constant such that the Hamming distance $H(\Sigma(\tau), \Sigma^{(\text{target})})$ is stationary for $t\tau_m + \tau_s \leq \tau < t\tau_m + \tau_m$. Another constant τ_m is set to $\tau_m = 2\tau_s$, which is found to range from 38 to 162 for $30 \leq N \leq 800$ in our simulations. If smaller values of τ_m and τ_s were used, $H_{G,t}^{(\text{target})}$ in Eq. (2) would not represent the adaptability of the network in the stationary state of the Boolean dynamics. The smaller $H_{G,t}^{(\text{target})}$ is, the closer the dynamical state on G is likely to approach the target state, implying that G is more adaptable to a given environment. We compute $H_{G',t}^{(\text{target})}$ in the same way as in Eq. (2).

The stability in performing routine processes is another key requirement of life. Given that local perturbations can spread globally, the ability to suppress such perturbation spread can be a measure of stability [23–31]. To quantify the stability of G at time t , the difference between the original state $\Sigma(\tau)$ and the perturbed state $\Sigma^{(\text{pert})}(\tau) = \{b_1^{(\text{pert})}(\tau), b_2^{(\text{pert})}(\tau), \dots, b_N^{(\text{pert})}(\tau)\}$ is measured. The perturbed state is obtained by flipping the states of $N/2$ randomly-selected b 's in $\Sigma(\tau)$ at $\tau = t\tau_m$ and then letting it evolve on G for $t\tau_m \leq \tau < (t+1)\tau_m$. Then we count the number of perturbed nodes, having $b_i \neq b_i^{(\text{pert})}$, as

$$H_{G,t}^{(\text{pert})} = \frac{1}{\tau_m - \tau_s} \sum_{\tau=t\tau_m+\tau_s}^{(t+1)\tau_m} H(\Sigma(\tau), \Sigma^{(\text{pert})}(\tau)) \quad (3)$$

with the Hamming distance $H(\Sigma, \Sigma^{(\text{pert})})$ defined in Eq. (2). $H_{G,t}^{(\text{pert})}$ represents the typical fraction of perturbed nodes; the smaller $H_{G,t}^{(\text{pert})}$ is, the more stable the network G is against dynamical perturbations. The stability of the mutant G' is also computed in the same way. We remark that the number of initial flipped variables can be changed over a significant range without changing the main results.

The mutant G' becomes the winner (i) if $H_{G',t}^{(\text{target})} < H_{G,t}^{(\text{target})}$ (G' is more adaptable than G) or (ii) if $H_{G',t}^{(\text{pert})} < H_{G,t}^{(\text{pert})}$ (G' is more stable than G) and $H_{G',t}^{(\text{target})} = H_{G,t}^{(\text{target})}$. If $H_{G',t}^{(\text{target})} = H_{G,t}^{(\text{target})}$ and $H_{G',t}^{(\text{pert})} = H_{G,t}^{(\text{pert})}$, the winner is chosen at random. Examples of the transition from G to G' are depicted in Fig. 1. Finally, to model the changes of the environment, a new target state $\Sigma^{(\text{target})'}$ is generated if $H^{(\text{target})}$ of the winner is zero. Therefore our network evolution model represents the co-evolution of the structure and dynamics of the Boolean network on different time scales in a changing environment.

III. EMERGENT FEATURES IN STRUCTURE AND FUNCTION

The simulation of the proposed model shows a variety of interesting features of evolving networks. Most of all, we find that the mean connectivity $\langle \bar{k}_t \rangle = \langle N^{-1} \sum_{i=1}^N k_i \rangle = \langle L_t \rangle / N$, with $k_i = \sum_{j=1}^N A_{ij}$ the in-degree or the number of regulators of node i and L_t the total number of links at time t , converges to a constant $\langle \bar{k}_\infty \rangle$, which depends only on N regardless of $\bar{k}_0 = L_0/N$ [Fig. 2 (a)]. The mean connectivity has been shown to converge to $\langle \bar{k}_\infty \rangle = 2$ in some evolution models [32, 34–36, 44], which is the critical point distinguishing the ordered and the chaotic phase in random Boolean networks [45]. Different values of $\langle \bar{k}_\infty \rangle$ have been reported in other models [26, 27], where $\langle \bar{k}_\infty \rangle > 2$, implying a fundamental difference between the evolved networks and random networks. In our model, $\langle \bar{k}_\infty \rangle$ ranges from 1.2 to 1.7 for $30 \leq N \leq 800$ and the data are fitted by a logarithmic growth with N as $\langle \bar{k}_\infty \rangle \sim 0.53 + 0.17 \ln N$ [See Fig. 2 (b)]. This suggests that $\langle \bar{k}_\infty \rangle$ would remain small for N reasonably large, e.g., $\langle \bar{k}_\infty \rangle \simeq 2.88$ for $N = 10^6$. Such sparse connectivity is identified in real biological networks [37–43]. The mean connectivities of the transcriptional regulatory networks are between 1 and 3 while the number of nodes ranges from hundreds to thousands. The mean connectivities of the metabolic bipartite networks also range between 1 and 3. Furthermore, they show logarithmic scaling with N in agreement with our model [See Fig. 2 (b)].

The number of regulator nodes (in-degree) k is broadly distributed in the evolved network compared with the Poissonian distribution of the random networks as seen in Fig. 2 (c). Such broad distributions are universally observed in real-world networks [2, 37, 41, 46, 47]. The cumulative in-degree distribution $C(k) = N^{-1} \sum_{i=1}^N \theta(k_i - k)$, with $\theta(x)$ the Heavisde step function, appear to take the form of an exponential function, which is in agreement with the transcriptional regulatory networks of *S. cerevisiae* [2, 41]. This is, however, inconsistent with the previous studies on the real metabolic networks [5] or other model networks evolving

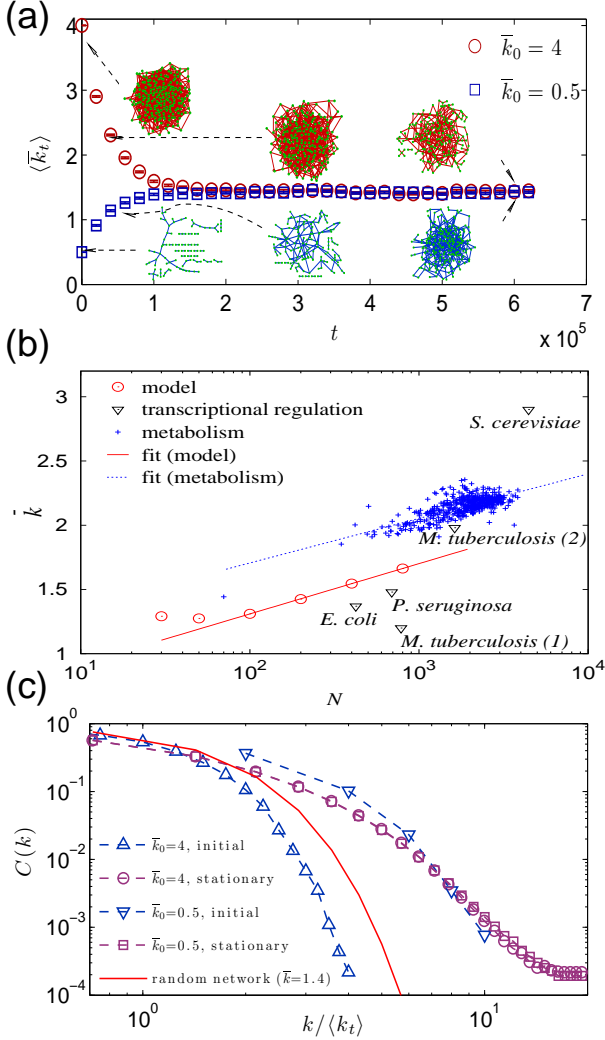


FIG. 2. (Color online) Emergence of a sparse and heterogeneous connectivity pattern. In simulations, the initial number of links L_0 is set to $4N$ or $N/2$ giving $\bar{k}_0 = L_0/N = 4$ or 0.5 . For each N and L_0 , we run \mathcal{N} independent simulations, each for $0 \leq t \leq T$, where T ranges from 4×10^4 to 5×10^6 and $\mathcal{N} = 1000$ for $N \leq 200$, $\mathcal{N} = 760$ for $N = 400$, and $\mathcal{N} = 22$ for $N = 800$. $\langle \dots \rangle$ indicates the ensemble average. (a) The plots of the mean connectivity $\langle \bar{k}_t \rangle$ for $N = 200$. It converges to a constant irrespective of the initial value, which is evaluated as $\langle \bar{k}_\infty \rangle = (T/4)^{-1} \sum_{t=(3/4)T}^T \langle \bar{k}_t \rangle \simeq 1.4$. The networks at selected times are presented. (b) The N -dependence of the stationary-state mean connectivity. $\langle \bar{k}_\infty \rangle \simeq 0.53 + 0.17 \ln N$ (solid line) fits reasonably the model results (circles). The mean connectivity $\bar{k} = L/N$ of the transcriptional regulatory networks of four species (triangles) [37–41] and of the bipartite metabolic networks of 506 species (crosses) [42, 43] are shown. The fitting line (dotted) given by $\langle \bar{k}_\infty \rangle \simeq 1.01 + 0.15 \ln N$ fits the data of the metabolic networks with N the number of reactions and metabolites. (c) The cumulative distributions of the in-degree, $C(k) = \langle N^{-1} \sum_{j=1}^N \theta(k_j - k) \rangle$ at $t = 0$ (initial state) and $t = 4.8 \times 10^5$ (stationary state) for $N = 200$. The distribution in the random networks of $N = 200$ nodes and $\langle L \rangle = \langle \bar{k}_\infty \rangle N = 1.4N$ links is also shown for comparison.

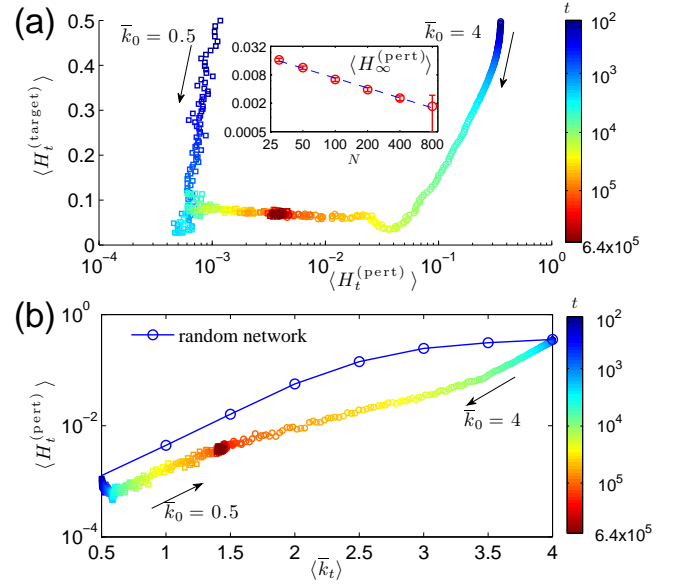


FIG. 3. (Color online) Time evolution of adaptability and stability. (a) Plot of $(\langle H_t^{(\text{pert})} \rangle, \langle H_t^{(\text{target})} \rangle)$ for $10^2 \leq t < 6.4 \times 10^5$ and $N = 200$ with the initial mean connectivity $\bar{k}_0 = 4$ and $\bar{k}_0 = 0.5$. $\mathcal{N} = 1000$ simulations are run. The color varies with the evolution time t and the arrows indicate the direction of increasing time. (Inset) The scaling behavior of the stationary-state Hamming distance $\langle H_\infty^{(\text{pert})} \rangle$ with respect to the number of nodes N . $\langle H_\infty^{(\text{pert})} \rangle \sim N^{-0.7}$ (dashed line) fits the data. (b) Plots of $\langle H_t^{(\text{pert})} \rangle$ versus the mean connectivity $\langle \bar{k}_t \rangle$ for the evolving networks and the random networks of $N = 200$.

via node duplication and divergence [32], which display power-law degree distributions. It is known that the node duplication [8] or the preferential attachment of links [10] may lead to such power-law degree distributions, which is missing in our model. In Ref. [48], the functional form of the degree distributions of some real metabolic networks are hard to point out.

In contrast to the broad in-degree distributions, the out-degree $k_i^{(\text{out})}$ in the evolved networks of our model is found to follow the Poisson distribution as in the random networks. It is known that the out-degree distribution is irrelevant to the determination of the dynamical phase - ordered or chaotic - of random Boolean networks [49].

As evolution proceeds, it is more facilitated for the evolving network to get close to or reach a given target state. Such adaptability is quickly acquired, as implied in the rapid decrease of $\langle H_t^{(\text{target})} \rangle$ with increasing t [Fig. 3 (a)]. We remark that $H_t^{(\text{target})}$ may increase with t even in a single realization of evolution, since the target state, the state demanded by the environment, may change with time. The extent of perturbation spread $\langle H_t^{(\text{pert})} \rangle$ also decreases rapidly by evolution. Its stationary-state value $\langle H_\infty^{(\text{pert})} \rangle$ shows the following scal-

ing behavior with N :

$$\langle H_{\infty}^{(\text{pert})} \rangle \sim N^{-\theta^{(\text{pert})}}, \quad \theta^{(\text{pert})} \simeq 0.7. \quad (4)$$

This implies an intermediate level of stability of the evolved networks compared with the following networks. The random Boolean networks with the mean connectivity at the threshold $\bar{k}_c = 2$ find the perturbation spread scale similarly to Eq. (4) but with a smaller scaling exponent ranging between $1/2$ and $1/3$, depending on the functional form of the in-degree distribution [49]. Therefore, the perturbation spread in those critical random networks is much larger than that in the evolved networks for large N . Figure 3 (b) shows that during the whole period of evolution, the evolving networks have smaller spread of perturbation than the random networks with the same mean connectivity $\langle \bar{k} \rangle$. On the other hand, in a variant of our model, the “stability-only” model, in which only the stability of the wild-type and the mutant is evaluated for selection, the perturbation spread scales as $\langle H_{\infty}^{(\text{pert})} \rangle \sim N^{-1}$ [Fig. 4 (b)]. The original networks allow larger spread of perturbation than the stability-only model in order to facilitate adaptation to a fluctuating environment.

The mean connectivity $\langle \bar{k}_{\infty} \rangle$ is also subject to such a balance constraint. As the opposite to the stability-only model, we can consider the “adaptation-only” model in which only the adaptability of the wild-type and the mutant is considered. We found that the mean connectivity is much larger than in the original model.¹ A large number of links make more and larger attractors in the state space, which can be helpful for adaptation. In the stability-only model, on the contrary, we find that the mean connectivity is much smaller than that of the original model [Fig. 4 (a)], suppressing the transitions between attractors. All these characteristics demonstrate that the structure and dynamics of the evolved networks are at the boundary between the stable and robust phase and the flexible and adaptable phase [15].

IV. A GENERALIZED MODEL

In this section, we represent our model in the Hamiltonian approach, which offers a natural extension of the model allowing us to check the robustness of the obtained results.

The evolution trajectory of the model network corresponds to a path in the space of networks G . A system of N nodes changes its location in the G space in the stochastic way as described in Sec. II. Therefore, a generalized evolution model can be introduced by specifying the transition probability $\omega_{G \rightarrow G'; \Sigma}$ from G to G'

¹ We found that the mean connectivity does not even become stationary but keeps increasing with time in some cases.

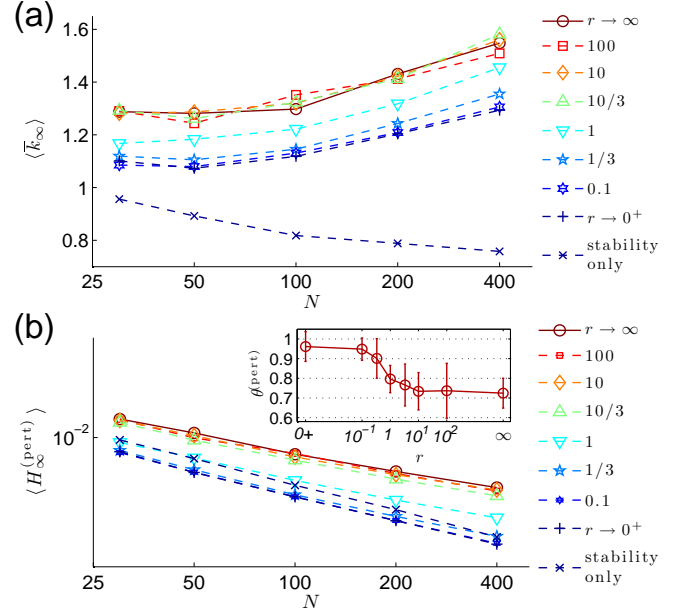


FIG. 4. (Color online) Mean connectivity and stability in the generalized model. The parameter r is related to the relative importance of adaptability with respect to stability as in Eq. (6). (a) Plots of the stationary-state mean connectivity $\langle \bar{k}_{\infty} \rangle$ versus the system size N . $\langle \bar{k}_{\infty} \rangle$ increases slowly with N for all $r > 0$ except for the stability-only model. (b) Plots of the perturbation spread $\langle H_{\infty}^{(\text{pert})} \rangle$ versus N . The scaling behavior $\langle H_{\infty}^{(\text{pert})} \rangle \sim N^{-\theta^{(\text{pert})}}$ is observed for all the considered cases. (Inset) the scaling exponent $\theta^{(\text{pert})}$ decreases from 1 to 0.7 with increasing r .

for a given dynamical state Σ [23, 26, 31]. Note that the dynamical state evolves with microscopic time τ in a deterministic way as long as the network structure G is fixed. Suppose that the transition probabilities satisfy the relation

$$\frac{\omega_{G \rightarrow G'; \Sigma}}{\omega_{G' \rightarrow G; \Sigma}} = \exp \left(-\frac{H_{G'}^{(\text{target})} - H_G^{(\text{target})}}{T^{(\text{target})}} - \frac{H_{G'}^{(\text{pert})} - H_G^{(\text{pert})}}{T^{(\text{pert})}} \right), \quad (5)$$

where the Hamming distances are computed by Eqs. (2) and (3) with $\Sigma(t\tau_m) = \Sigma$ and two temperatures $T^{(\text{target})}$ and $T^{(\text{pert})}$ are introduced. Transitions to the networks with smaller $H^{(\text{target})}$ and $H^{(\text{pert})}$ are preferred to the extent depending on the two temperatures. Our model corresponds to the limit

$$T^{(\text{target})} \rightarrow 0, \quad T^{(\text{pert})} \rightarrow 0, \quad \text{and} \quad r \equiv \frac{T^{(\text{pert})}}{T^{(\text{target})}} \rightarrow \infty, \quad (6)$$

since the transition from G to G' is made only if $H_{G'}^{(\text{target})} < H_G^{(\text{target})}$ or $H_{G'}^{(\text{target})} = H_G^{(\text{target})}$ and $H_{G'}^{(\text{pert})} \leq H_G^{(\text{pert})}$. In case $T^{(\text{target})} > 0$ and $T^{(\text{pert})} > 0$, the transition to a less adaptable ($H^{(\text{target})}$ -larger) or

less stable ($H^{(\text{pert})}$ -larger) network can be made with non-zero probability contrary to that of our model. The adaptability-only model corresponds to the limit $T^{(\text{target})} \rightarrow 0$ and $T^{(\text{pert})} \rightarrow \infty$ and the stability-only model to $T^{(\text{target})} \rightarrow \infty$ and $T^{(\text{pert})} \rightarrow 0$.

With the transition probabilities satisfying Eq. (5), each network G appears in the stationary state with probability

$$P_{G;\Sigma} \propto \exp \left(-\frac{H_G^{(\text{target})}}{T^{(\text{target})}} - \frac{H_G^{(\text{pert})}}{T^{(\text{pert})}} \right), \quad (7)$$

with the two Hamming distances playing the role of Hamiltonians coupled with two temperatures.

To investigate the robustness of the results obtained in Sec. III, we investigate this generalized model with the temperature ratio r positive, $T^{(\text{pert})} \rightarrow 0$, and $T^{(\text{target})} \rightarrow 0$. For $r > 0$, the transition from G to G' is available if and only if $H_{G'}^{(\text{pert})} + rH_{G'}^{(\text{target})} \leq H_G^{(\text{pert})} + rH_G^{(\text{target})}$. r controls the relative importance of $H^{(\text{target})}$ with respect to $H^{(\text{pert})}$. Simulations show that $\langle \bar{k}_\infty \rangle$ displays similar N -dependent behaviors for all $r > 0$; it increases with N slowly [See. Fig. 4(a)]. On the contrary, in the stability-only model, the mean connectivity decreases with N . This highlights the crucial role of adaptation in shaping the architecture of regulatory networks. Secondly, as shown in Fig. 4 (b), $\langle H_\infty^{(\text{pert})} \rangle \sim N^{-\theta^{(\text{pert})}}$ with $\theta^{(\text{pert})} \simeq 0.7$ is observed not only for $r \rightarrow \infty$ but also for sufficiently large r , in the range $r \gtrsim 10$. For small r , roughly $r \lesssim 0.1$ and in the stability-only model, $\langle H_\infty^{(\text{pert})} \rangle \sim N^{-1}$, implying that stronger stability is achieved than for large r . The scaling exponent $\theta^{(\text{pert})}$ decreases from 1 to 0.7 with r increasing in the range $0.1 \lesssim r \lesssim 10$. Such robustness of the structural and functional properties for all large r makes our model ($r \rightarrow \infty$) appropriate for modeling the evolutionary selection requesting both adaptability and stability.

V. SCALING OF FLUCTUATION

As the initial randomly-wired networks evolve, many of their properties change with time, the investigation of which may illuminate the mechanisms of evolution by which living organisms optimize their architecture for acquiring adaptability and stability.

Evolution is accompanied by fluctuations. Environments are different for different groups of organisms and vary with time as well even for a given group. Mutants are generated at random and thus the specific pathway of evolution becomes stochastic. The studied networks also display fluctuations over different realizations of evolution $\sigma = \sqrt{\langle A^2 \rangle - \langle A \rangle^2}$ for each quantity A . Among others, here we investigate such ensemble fluctuation of perturbation spread characterizing the system's stability $\sigma_t = \sqrt{\langle (H_t^{(\text{pert})})^2 \rangle - \langle H_t^{(\text{pert})} \rangle^2}$. While

the evolutionary pressure results in enhancing stability (reducing $\langle H^{(\text{pert})} \rangle$), its fluctuation, normalized by the mean $\langle H^{(\text{pert})} \rangle$, is stronger and the whole distribution is broader, respectively, than those of random networks as shown in Fig. 5 (a). Such enhancement of fluctuations helps the evolving network search for the optimal topology under fluctuating environments [50–53].

It is observed for a wide range of real-world systems that the standard deviation σ and the mean m of a dynamic variable show the scaling relation $\sigma \sim m^\alpha$ with the scaling exponent α reflecting the nature of the dynamical processes: For instance, $\alpha = 1/2$ in the case of no correlations among the relevant variables and their distributions having finite moments as in the conventional random walk while the widely varying external influence may make such significant correlations as leading to $\alpha \neq 1/2$ [54–57]. Such scaling relation has been observed for the gene expression level or the protein concentration that fluctuates over cells and time [58, 59]. Also in our model the mean $\langle H_t^{(\text{pert})} \rangle$ and the fluctuation σ_t of perturbation spread at different times t satisfy the scaling relation

$$\sigma_t \sim \langle H_t^{(\text{pert})} \rangle^\alpha. \quad (8)$$

Interestingly, the scaling exponent α changes with evolution [Fig. 5 (b)]; $\alpha = \alpha_{\text{tr}}$ with $\alpha_{\text{tr}} \simeq 0.5$ for $k_0 = 4$ and $\alpha_{\text{tr}} \simeq 0.6$ for $k_0 = 0.5$ during transient period but $\alpha = \alpha_{\text{st}}$ with $\alpha_{\text{st}} \simeq 1$ in the stationary state. Such crossover in α is robustly observed for all N and L_0 as shown in Fig. 5(c) and 5(d).

What is the origin of such dynamic crossover in α ? It has been shown that the interplay of exogenous and endogenous dynamics may affect the scaling exponent α in systems under the influence of external environments [54–57, 60, 61]. In our evolution model, the extent of perturbation spread depends on the initial perturbation and on the network structure. The network structure is the outcome of the specific evolution pathway affected by the changing environment. The location of initial perturbation is determined on a random basis in our model, modeling the stochasticity of the internal microscopic dynamics in real systems. Therefore the perturbation spread can be considered as a function of the internal dynamics component D and the network structure S , i.e., $H^{(\text{pert})}(D, S)$. Then the fluctuation of $H^{(\text{pert})}$ is represented as $\sigma^2 = \langle \langle H^{(\text{pert})2} \rangle_D \rangle_S - \langle \langle H^{(\text{pert})} \rangle_D \rangle_S^2$, where $\langle \dots \rangle_D$ and $\langle \dots \rangle_S$ represent the average over D and S as $\int dD P(D) \dots$ and $\int dS P(S) \dots$ and decomposed into the internal and the external fluctuation as [60, 61]:

$$\begin{aligned} \sigma^2 &= \sigma^{(I)2} + \sigma^{(E)2}, \\ \sigma^{(I)} &= \sqrt{\langle \langle H^{(\text{pert})2} \rangle_D \rangle_S - \langle \langle H^{(\text{pert})} \rangle_D \rangle_S^2}, \\ \sigma^{(S)} &= \sqrt{\langle \langle H^{(\text{pert})} \rangle_D^2 \rangle_S - \langle \langle H^{(\text{pert})} \rangle_D \rangle_S^2}. \end{aligned} \quad (9)$$

The internal fluctuation $\sigma^{(I)}$ denotes the structural average of the internal-dynamics fluctuation of $H^{(\text{pert})}$.

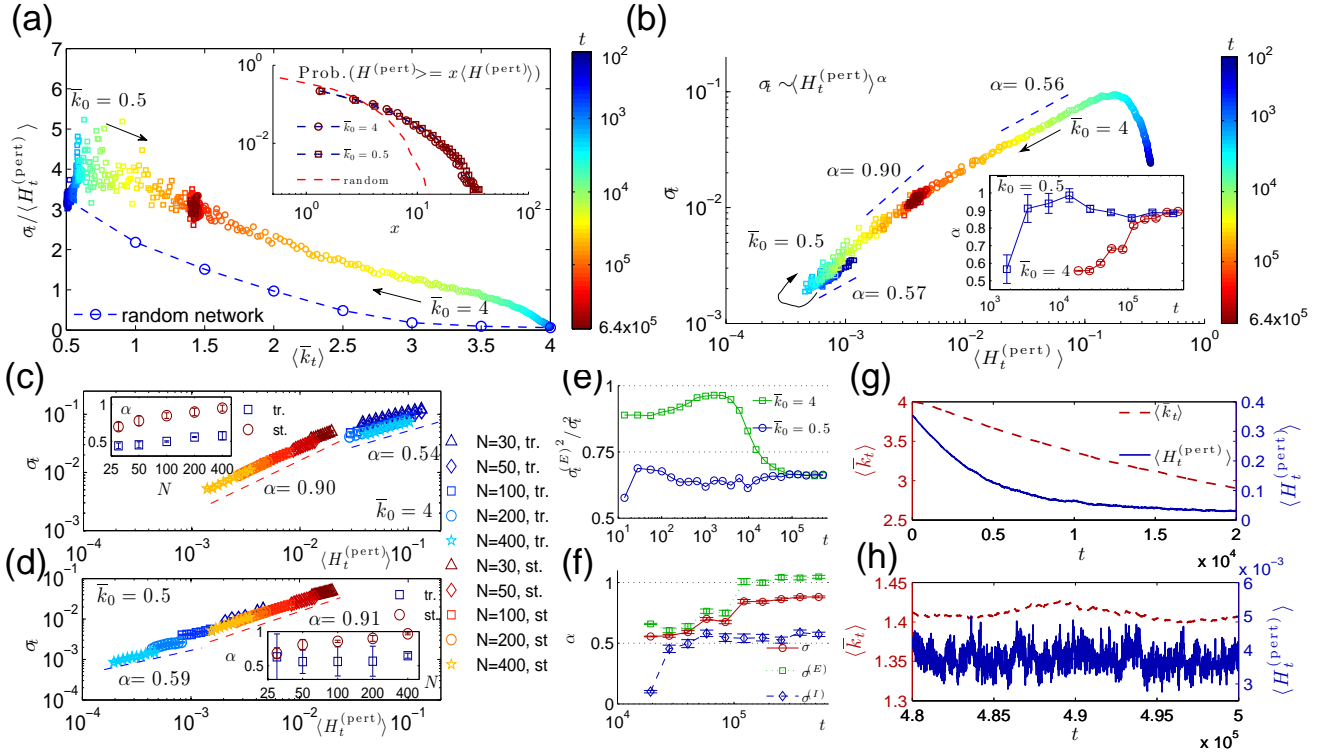


FIG. 5. (Color online) Scaling behaviors of fluctuation of perturbation spread. (a) The normalized fluctuation $\sigma_t / \langle H_t^{(\text{pert})} \rangle$ as a function of the mean connectivity $\langle k_t \rangle$ for $N = 200$. It is larger than that in the random networks (dashed line). The color varies with the evolution time t and the arrows indicate the direction of increasing time. (Inset) The cumulative distributions of $H_{G,t}^{(\text{pert})}$ in the stationary state ($t > 4.8 \times 10^5$) compared with those of the random networks of $\langle k \rangle = 1.4$ (dashed line). (b) Plots of σ_t with respect to $\langle H_t^{(\text{pert})} \rangle$ for $\bar{k}_0 = 4$ and 0.5 and $N = 200$. (Inset) The estimated scaling exponents α in Eq. (8) as functions of time t . (c) Plots of σ_t versus the log-binned values of $\langle H_t^{(\text{pert})} \rangle$ in the transient (tr.) and stationary (st.) periods for system sizes $N = 50, 100, 200$, and 400 with $\bar{k}_0 = 4$. The slopes of the two fitting lines, 0.90 and 0.54 , are the averages of the estimated exponents α in the transient and the stationary period, respectively. (Inset) Plots of α versus N in the transient and the stationary period. (d) The same plots as (c) with $\bar{k}_0 = 0.5$. The slopes, 0.91 and 0.59 , of the two fitting lines are the average of α for $N = 50, 100, 200$, and 400 . (Inset) Plots of α versus N in the transient and the stationary periods. (e) The ratio $\sigma_t^{(E)2} / \sigma_t^2$ as functions of time t for $\bar{k}_0 = 4$ and 0.5 . In the stationary state, $\sigma_t^{(E)2} / \sigma_t^2 \simeq 0.67$ without regards to the initial mean connectivity or the system size. (f) The estimated scaling exponents α for the whole, external, and internal fluctuation at each time t for $N = 200$. (g) Plots of $\langle H_t^{(\text{pert})} \rangle$ and $\langle k_t \rangle$ versus time t in the transient period $0 < t < 20,000$. Both decrease with little fluctuation. (h) Plots of $\langle H_t^{(\text{pert})} \rangle$ and $\langle k_t \rangle$ versus t in the stationary period $480,000 < t < 500,000$. The larger fluctuation of $\langle H_t^{(\text{pert})} \rangle$ than $\langle k_t \rangle$ is seen.

On the other hand, the external fluctuation $\sigma^{(E)}$ is the structural fluctuation of the internal-dynamics average of $H^{(\text{pert})}$. In simulations, the quantities $\langle \langle \dots \rangle_D \rangle_S$ are obtained simply by the ensemble averages $\langle \dots \rangle$. To obtain $\langle \langle H^{(\text{pert})} \rangle_D^2 \rangle_S$, we use the relation $\langle \langle H^{(\text{pert})} \rangle_D^2 \rangle_S = \langle H^{(\text{pert},I)} H^{(\text{pert},II)} \rangle$ [60, 61], where $H^{(\text{pert},I)}$ and $H^{(\text{pert},II)}$ are the perturbation spreads from two different initial perturbations on the same network and are computed by Eq. (3) with different perturbed states $\Sigma^{(\text{pert},I)}$ and $\Sigma^{(\text{pert},II)}$ from two initial perturbations. Inserting $\langle H^{(\text{pert})2} \rangle = (1/2)(\langle H^{(\text{pert},I)2} \rangle + \langle H^{(\text{pert},II)2} \rangle)$ and $\langle H^{(\text{pert})} \rangle = (1/2)(\langle H^{(\text{pert},I)} \rangle + \langle H^{(\text{pert},II)} \rangle)$ in Eq. (9), one finds that the internal fluctuation is represented as $\sigma^{(I)2} = (1/2)\langle (H^{(\text{pert},I)} - H^{(\text{pert},II)})^2 \rangle$ and the external

fluctuation is $\sigma^{(E)2} = \langle (H^{(\text{pert},I)} - \langle H^{(\text{pert},I)} \rangle)(H^{(\text{pert},II)} - \langle H^{(\text{pert},II)} \rangle) \rangle$.

The external fluctuation $\sigma_t^{(E)}$ is found to be much larger than $\sigma_t^{(I)}$ for all t [Figure 5 (e)], implying the wide variation of the network structure arising from exploiting differentiated pathways of evolution in changing environments. Moreover, the external fluctuation displays a similar crossover behavior to σ_t , that is, $\sigma_t^{(E)} \sim \langle H_t^{(\text{pert})} \rangle^{\alpha^{(E)}}$ with $\alpha^{(E)}$ increasing from $\alpha_{\text{tr}}^{(E)}$, a value close to $1/2$, in the transient period to a value $\alpha_{\text{st}}^{(E)} \simeq 1$ in the stationary state [Fig. 5 (f)]. On the other hand, the internal fluctuation behaves as $\sigma_t^{(I)} \sim \langle H_t^{(\text{pert})} \rangle^{\alpha^{(I)}}$ with $\alpha^{(I)}$ remaining close to $1/2$, like in the diffusion process [Fig. 5(f)].

Which is dominant of the internal and the external

fluctuation has been investigated for various complex systems [54–57]. Contrary to the static (nature of) systems of the previous works, the evolving networks in our model display a dynamic crossover in the fluctuation scaling while the external fluctuation is always dominant. To decipher the mechanism underlying this phenomenon, we begin with assuming that in the scaling regime the perturbation spread $H_t^{(\text{pert})}$ is small and factorized as

$$H_t^{(\text{pert})} \simeq D_t S_t, \quad (10)$$

where D_t and S_t are the components reflecting the dependence of perturbation spread on the location of initial perturbation and on the global network structure, respectively. D_t and S_t are expected to be independent. We assume that their fluctuations scale as $\xi_t^{(D)} = \sqrt{\langle D_t^2 \rangle - \langle D_t \rangle^2} \sim \langle D_t \rangle^{\beta^{(D)}}$ and $\xi_t^{(S)} = \sqrt{\langle S_t^2 \rangle - \langle S_t \rangle^2} \sim \langle S_t \rangle^{\beta^{(S)}}$ with $\beta^{(D)}$ and $\beta^{(S)}$ time-independent constants. Then the mean of the perturbation spread should be given by

$$\langle H_t^{(\text{pert})} \rangle = \langle D_t \rangle \langle S_t \rangle \quad (11)$$

and the internal and the external fluctuation in Eq. (9) are represented as

$$\begin{aligned} \sigma_t^{(I)} &= \sqrt{(\langle D_t^2 \rangle - \langle D_t \rangle^2) \langle S_t^2 \rangle} \sim \langle D_t \rangle^{\beta^{(D)}} \sqrt{\langle S_t^2 \rangle}, \\ \sigma_t^{(E)} &= \langle D_t \rangle \sqrt{\langle S_t^2 \rangle - \langle S_t \rangle^2} \sim \langle D_t \rangle \langle S_t \rangle^{\beta^{(S)}}. \end{aligned} \quad (12)$$

Using Eqs. (11) and (12), we can analyze the scaling behaviors of fluctuations as follows. In the transient period before entering the stationary state, the network structure is transformed significantly, making the structural component $\langle S_t \rangle$ essentially govern the perturbation spread in its time-dependent behavior, yielding

$$\langle H_t^{(\text{pert})} \rangle \sim \langle S_t \rangle, \quad \sigma_t^{(I)} \sim \sqrt{\langle S_t^2 \rangle}, \quad \sigma_t^{(E)} \sim \langle S_t \rangle^{\beta^{(S)}}. \quad (13)$$

This is supported by the similarity of the temporal patterns of $\langle H_t^{(\text{pert})} \rangle$ and the mean connectivity $\langle k_t \rangle$ in Fig. 5 (g). Therefore one can relate the external fluctuation to the mean of perturbation spread as

$$\sigma_t^{(E)} \sim \langle S_t \rangle^{\beta^{(S)}} \sim \langle H_t^{(\text{pert})} \rangle^{\beta^{(S)}}. \quad (14)$$

Comparing this with the simulation results in Fig. 5(f), we find that $\beta^{(S)} \simeq \alpha_{\text{tr}}^{(E)} \simeq 1/2$. That is, $\xi^{(S)} \sim \langle S \rangle^{1/2}$. The estimated value $\beta^{(S)}$ is also consistent with the simulation result $\alpha_{\text{tr}}^{(I)} \simeq 1/2$, since $\sigma_t^{(I)} \sim \sqrt{\langle S_t^2 \rangle} \sim \sqrt{\langle S_t \rangle^2 + (\text{const.}) \langle S_t \rangle^{2\beta^{(S)}}} \sim \langle S_t \rangle^{\beta^{(S)}}$, with $\langle S_t \rangle \ll 1$ given $\langle H^{(\text{pert})} \rangle$ small in the scaling regime.

In the stationary state, the network structure varies little with time; $\langle k_t \rangle$ rarely varies (Fig. 5 (h)). In contrast, $\langle H_t^{(\text{pert})} \rangle$ fluctuates significantly on short time scales. This suggests that randomly-selected locations of initial perturbation, having no correlations at different time

steps, drive such time-dependent behaviors of $\langle H_t^{(\text{pert})} \rangle$. Therefore, from Eqs. (11) and (12), the mean and the fluctuation of perturbation spread are represented as

$$\langle H_t^{(\text{pert})} \rangle \sim \langle D_t \rangle, \quad \sigma_t^{(I)} \sim \langle D_t \rangle^{\beta^{(D)}}, \quad \sigma_t^{(E)} \sim \langle D_t \rangle. \quad (15)$$

Regardless of the value of $\beta^{(D)}$, the external fluctuation is proportional to $\langle H_t^{(\text{pert})} \rangle$,

$$\sigma_t^{(E)} \sim \langle D_t \rangle \sim \langle H_t^{(\text{pert})} \rangle \quad (16)$$

in agreement with the observation $\alpha_{\text{st}}^{(E)} \simeq 1$ in Fig. 5 (f). The internal fluctuation is expected to scale as $\sigma_t^{(I)} \sim \langle D_t \rangle^{\beta^{(D)}} \sim \langle H_t^{(\text{pert})} \rangle^{\beta^{(D)}}$, which allows us to find $\beta^{(D)} \simeq \alpha^{(I)} \simeq 1/2$. Therefore $\xi^{(D)} \sim \langle D \rangle^{1/2}$ like $\xi^{(S)} \sim \langle S \rangle^{1/2}$.

The above arguments following Eqs. (11) and (12) with $\beta^{(S)} \simeq \beta^{(D)} \simeq 1/2$ illustrate why the internal fluctuation always scale as $\sigma_t^{(I)} \sim \langle H_t^{(\text{pert})} \rangle^{1/2}$ while the external fluctuation shows the dynamic crossover from $\sigma_t^{(E)} \sim \langle H_t^{(\text{pert})} \rangle^{1/2}$ to $\sigma_t^{(E)} \sim \langle H_t^{(\text{pert})} \rangle$. Combined with the observation that the external fluctuation makes a dominant contribution to σ_t , the arguments explain the crossover in the fluctuation scaling of perturbation spread shown in Fig. 5 (b).

Our results can be compared with the other cases showing a crossover in the fluctuation scaling driven by the change of the dominant fluctuation between $\sigma^{(I)}$ and $\sigma^{(E)}$ [56]. On the other hand, $\sigma^{(E)}$ is always dominant in our model. The time-varying perturbation spread is dominantly governed by the structure component S_t in the transient period and the internal dynamics component D_t in the stationary state, which underlies the crossover of α from 1/2 to 1 in our model. The rapid and significant changes of the structure of the evolving networks are identified only in the transient period, and the internal stochasticity dominates the statistics of stability in the stationary state of evolution. Therefore the nature of fluctuations is fundamentally different between the evolved networks and the random network or those which are not sufficiently evolved.

VI. CORRELATION VOLUME

The evolved networks in our model are more stable than random networks but less stable than the stability-only networks as shown by the scaling behaviors of $\langle H_\infty^{(\text{pert})} \rangle$ in Sec. III. Such balance between robustness and flexibility is hardly acquired unless the relevant dynamical variables, the spread of perturbation in our case, at different sites are correlated with one another.

For a quantitative analysis, let us consider the local perturbation $h_{i,t}$ at node i and time t defined as

$$h_{i,t} = \frac{1}{\tau_m - \tau_s} \sum_{\tau=t\tau_m+\tau_s}^{(t+1)\tau_m} \left[1 - \delta_{b_i(\tau), b_i^{(\text{pert})}(\tau)} \right], \quad (17)$$

denoting whether the activity of node i is different between the original state Σ and the perturbed state $\Sigma^{(\text{pert})}$. Notice that the stability Hamming distance $H_t^{(\text{pert})}$ in Eq. (3) is the spatial average of the local perturbations, $H_t^{(\text{pert})} = N^{-1} \sum_{i=1}^N h_{i,t}$. If node j tends to have larger perturbation than its average when node i does, $h_{i,t} > \langle h_{i,t} \rangle$, their local perturbations can be considered as correlated, meaning that local fluctuations at $i(j)$ are likely to spread to node $j(i)$. In that case, we can expect that $\langle (h_{i,t} - \langle h_{i,t} \rangle)(h_{j,t} - \langle h_{j,t} \rangle) \rangle = \langle h_{i,t} h_{j,t} \rangle - \langle h_{i,t} \rangle \langle h_{j,t} \rangle > 0$. Therefore we define the correlation volume as

$$C_t \equiv \frac{\sum_{i=1}^N \sum_{j \neq i} (\langle h_{i,t} h_{j,t} \rangle - \langle h_{i,t} \rangle \langle h_{j,t} \rangle)}{\sum_{j=1}^N (\langle h_{j,t}^2 \rangle - \langle h_{j,t} \rangle^2)}, \quad (18)$$

which represents how many nodes are correlated with a node in the perturbation-spreading dynamics. For instance, $C_t = N - 1$ if $h_{i,t} = h_{j,t}$ for all i and j (perfect correlation) and $C_t = 0$ if the h 's are completely independent of one another such that $\langle h_{i,t} h_{j,t} \rangle = \langle h_{i,t} \rangle \langle h_{j,t} \rangle$.

One can find that the variance of the perturbation spread $\sigma_t^2 = \langle H_t^{(\text{pert})2} \rangle - \langle H_t^{(\text{pert})} \rangle^2$ is decomposed into the local variance \mathcal{S}_t and the correlation volume C_t as

$$\sigma_t^2 = \mathcal{S}_t(1 + C_t), \quad (19)$$

where \mathcal{S}_t is defined in terms of the variance of $h_{i,t}$ as

$$\mathcal{S}_t \equiv \frac{1}{N^2} \sum_{i=1}^N (\langle h_{i,t}^2 \rangle - \langle h_{i,t} \rangle^2). \quad (20)$$

The decomposition in Eq. (19) allows us to see that the fluctuation of perturbation spread depends on the magnitude of local fluctuations, \mathcal{S}_t , and how far the local fluctuation propagates to the system, characterized by the correlation volume C_t in Eq. (18). If the $h_{i,t}$'s are independent, the local fluctuation does not spread, as $C_t = 0$, and the whole variance σ_t^2 is identical to the local variance $\sigma_t^2 = \mathcal{S}_t$. On the contrary, if the $h_{i,t}$'s are perfectly correlated, the correlation volume is $N - 1$ and the whole variance σ_t^2 is N times larger than the local variance as $\sigma_t^2 = N\mathcal{S}_t$, representing that local fluctuations spread to the whole system.

In Fig. 6 (a), the correlation volume is shown to be larger in the stationary state than in the initial state. The correlation volume averaged over the stationary period, C_∞ , is about 10 while that in the initial state, C_0 , ranges between 2 and 3 for $N = 200$. The dependence of C_t on the system size N is different between the initial and the stationary states. Furthermore, the correlation volume in the stationary state increases with N as

$$C_\infty \sim N^\zeta \text{ with } \zeta \simeq 0.4 \quad (21)$$

while the correlation volume of the initial network C_0 does not increase with N [Fig. 6 (b)]. Such a scaling behavior is not seen in the whole fluctuation σ_t^2 even in the evolved networks. Therefore, the scaling behavior of the correlation volume in Eq. (21) can be another hallmark of the evolved systems and can be related to the system's capacity to be stable and adaptable simultaneously.

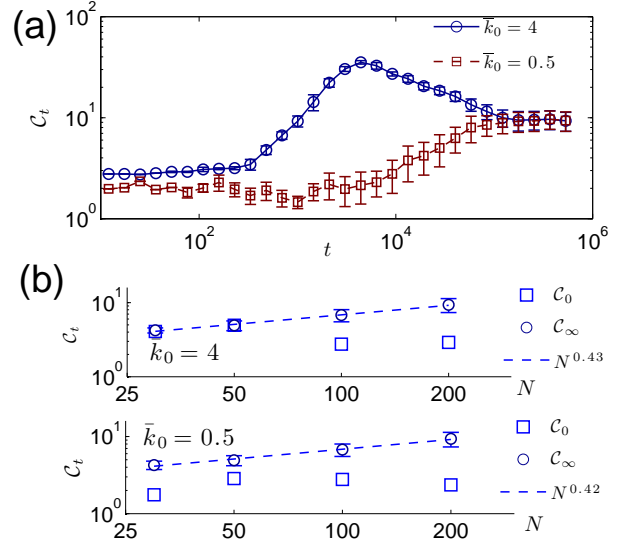


FIG. 6. (Color online) Correlation volume C_t . (a) Plots of C_t versus time t for $N = 200$. (b) The initial correlation volume C_0 at $t = 0$ and the stationary-state one C_∞ averaged over the stationary period ($t > 4.8 \times 10^5$) are plotted as functions of the system size N for $\bar{k}_0 = 4$ (upper) and for $\bar{k}_0 = 0.5$ (lower). C_∞ scales with N as $C_\infty \sim N^{0.43}$ or $N^{0.42}$ while C_0 does not increase with N .

VII. SUMMARY AND DISCUSSION

In this work we have introduced and extensively investigated the characteristic properties of an adaptive network model capturing the generic features of biological evolution. In reality, the evolutionary selections are made for a population of heterogeneous living organisms, as adopted by the genetic algorithm, but here we considered a simplified model, where a single network, representing the network structure typical of a population of organisms, add or remove a link depending on whether that change improves its fitness or not. The fitness of a network is evaluated in terms of its adaptability to a changing environment and the stability against perturbations in the dynamical state, which look contradictory to each other but essential for every living organism. Despite such simplification, the model network reproduces many of the universal network characteristics of evolving organisms, including the sparsity and scaling of the mean connectivity, broad degree distributions, and stability stronger than the random Boolean networks but weaker than the networks evolved towards stability only, implying the simultaneous support of adaptability and robustness.

Fluctuations and correlations display characteristic scaling behaviors in the stationary state of evolution contrasted to those in the transient period or in the initial random-network state. The evolutionary pressure drives the regulatory networks towards becoming highly stable by exploiting different pathways from realization to realization in the rugged fitness landscape, which results in

a large fluctuation. The presence of two distinct components in the perturbation-spread dynamics, related to the different network structure depending on the evolution pathway and the location of random initial perturbation, respectively, is shown to bring the dynamic crossover in the fluctuation scaling. Such evolution makes large correlations as well.

The proposed model is simple and generic allowing us to understand the evolutionary origin of the universal features of diverse biological networks. It illuminates the nature of dynamic fluctuations and correlations in evolving networks that are continuously influenced by the changing environments. The ensemble of those evolving networks can be formulated by the Hamiltonian approach, which depends on a time-varying external environment, and thus it opens a way to study biological evolution

from the viewpoint of statistical mechanics. Given the increasing importance of the capacity to manipulate biological systems, natural or synthetic, our understanding of biological fluctuations can be particularly useful. The strong interaction with environments, like the natural selection in evolution, is common to diverse complex systems and thus the theoretical framework to deal with multiple components of dynamics presented here can be of potential use in substantiating the theory of complex systems.

ACKNOWLEDGMENTS

This work was supported by the National Research Foundation of Korea (NRF) grant funded by the Korean Government (MSIP) (No. 2013R1A2A2A01068845).

-
- [1] A.-L. Barabasi and Z. N. Oltvai, *Nat. Rev. Genet.* **5**, 101 (2004).
 - [2] T. I. Lee *et al.*, *Science* **298**, 799 (2002).
 - [3] J.-F. Rual *et al.*, *Nature* **437**, 1173 (2005).
 - [4] H. Ma and A.-P. Zeng, *Bioinformatics* **19**, 270 (2003).
 - [5] H. Jeong, B. Tombor, R. Albert, Z. N. Oltvai, and A. L. Barabasi, *Nature* **407**, 651 (2000).
 - [6] S. S. Shen-Orr, R. Milo, S. Mangan, and U. Alon, *Nat. Genet.* **31**, 64 (2002).
 - [7] A.-L. Barabási and R. Albert, *Science* **286**, 509 (1999).
 - [8] A. Vázquez, A. Flammini, A. Maritan, and A. Vespignani, *Complexus* **1**, 38 (2003).
 - [9] T. Yamada and P. Bork, *Nat. Rev. Mol. Cell Biol.* **10**, 791 (2009).
 - [10] A.-L. Barabási, R. Albert, and H. Jeong, *Physica A* **272**, 173 (1999).
 - [11] R. Fisher and H. Bennett, *The Genetical Theory of Natural Selection: A Complete Variorum Edition* (OUP Oxford, 1999).
 - [12] H. A. Orr, *Nat. Rev. Genet.* **6**, 119 (2005).
 - [13] A. Wagner, *Robustness and Evolvability in Living Systems* (Princeton Univ. Press, Princeton, 2005).
 - [14] H. J. Beaumont, J. Gallie, C. Kost, G. C. Ferguson, and P. B. Rainey, *Nature* **462**, 90 (2009).
 - [15] S. Kauffman, *J. Theor. Biol.* **22**, 437 (1969).
 - [16] M. M. Babu, N. M. Luscombe, L. Aravind, M. Gerstein, and S. A. Teichmann, *Curr. Opin. Struct. Biol.* **14**, 283 (2004).
 - [17] C.-M. Ghim, K.-I. Goh, and B. Kahng, *J. Theor. Biol.* **237**, 401 (2005).
 - [18] S. A. Kauffman and R. G. Smith, *Physica D* **22**, 68 (1986).
 - [19] M. Stern, *Proc. Nat'l. Acad. Sci. U.S.A.* **96**, 10746 (1999).
 - [20] P. Oikonomou and P. Cluzel, *Nat. Phys.* **2**, 532 (2006).
 - [21] F. Stauffer and J. Berg, *EPL* **88**, 48004 (2009).
 - [22] S. F. Greenbury, I. G. Johnston, M. A. Smith, J. P. Doye, and A. A. Louis, *J. Theor. Biol.* **267**, 48 (2010).
 - [23] A. Wagner, *Evolution* **50**, 1008 (1996).
 - [24] S. Bornholdt and K. Sneppen, *Phys. Rev. Lett.* **81**, 236 (1998).
 - [25] A. Szejkka and B. Drossel, *Eur. Phys. J. B* **56**, 373 (2007).
 - [26] V. Sevim and P. A. Rikvold, *J. Theor. Biol.* **253**, 323 (2008).
 - [27] C. Fretter, A. Szejkka, and B. Drossel, *New J. Phys.* **11**, 033005 (2009).
 - [28] A. Esmaeili and C. Jacob, *Biosystems* **98**, 127 (2009).
 - [29] T. Mihaljev and B. Drossel, *Eur. Phys. J. B* **67**, 259 (2009).
 - [30] A. Szejkka and B. Drossel, *Phys. Rev. E* **81**, 021908 (2010).
 - [31] T. P. Peixoto, *Phys. Rev. E* **85**, 041908 (2012).
 - [32] C. Torres-Sosa, S. Huang, and M. Aldana, *PLoS Comput. Biol.* **8**, e1002669 (2012).
 - [33] S. Bornholdt and T. Rohlf, *Phys. Rev. Lett.* **84**, 6114 (2000).
 - [34] T. Rohlf, N. Gulbahce, and C. Teuscher, *Phys. Rev. Lett.* **99**, 248701 (2007).
 - [35] T. Rohlf, *EPL* **84**, 10004 (2008).
 - [36] M. Liu and K. E. Bassler, *Phys. Rev. E* **74**, 041910 (2006).
 - [37] G. Balázsi, A.-L. Barabási, and Z. Oltvai, *Proc. Nat'l. Acad. Sci. U.S.A.* **102**, 7841 (2005).
 - [38] E. Galán-Vázquez, B. Luna, and A. Martínez-Antonio, *Microb. Inform. Exp.* **1**, 3 (2011).
 - [39] G. Balázsi, A. P. Heath, L. Shi, and M. L. Gennaro, *Mol. Sys. Biol.* **4**, 225 (2008).
 - [40] J. Sanz, J. Navarro, A. Arbués, C. Martín, P. C. Marijuán, and Y. Moreno, *Plos One* **6**, e22178 (2011).
 - [41] S. Balaji, M. M. Babu, L. M. Iyer, N. M. Luscombe, and L. Aravind, *J. Mol. Biol.* **360**, 213 (2006).
 - [42] P. D. Karp *et al.*, *Nucleic Acids Research* **33**, 6083 (2005).
 - [43] P. Kim, D.-S. Lee, and B. Kahng, (unpublished).
 - [44] A. Goudarzi, C. Teuscher, N. Gulbahce, and T. Rohlf, *Phys. Rev. Lett.* **108**, 128702 (2012).
 - [45] B. Derrida and Y. Pomeau, *Europhys. Lett.* **1**, 45 (1986).
 - [46] R. Albert and A.-L. Barabási, *Rev. Mod. Phys.* **74**, 47 (2002).
 - [47] D. Thieffry, A. M. Huerta, E. Pérez-Rueda, and J. Collado-Vides, *Bioessays* **20**, 433 (1998).
 - [48] A. Clauset, C. Shalizi, and M. Newman, *SIAM Review* **51**, 661 (2009).
 - [49] D.-S. Lee and H. Rieger, *J. Phys. A: Math. Theor.* **41**, 415001 (2008).

- [50] A. Eldar and M. Elowitz, *Nature* **467**, 167 (2010).
- [51] E. Kussel and S. Leibler, *Science* **309**, 2075 (2005).
- [52] M. Thattai and A. van Oudenaarden, *Genetics* **167**, 523 (2004).
- [53] D. Wolf, V. Vazirani, and A. Arkin, *J. Theor. Biol.* **234**, 227 (2005).
- [54] M. A. de Menezes and A.-L. Barabási, *Phys. Rev. Lett.* **92**, 028701 (2004).
- [55] M. A. de Menezes and A.-L. Barabási, *Phys. Rev. Lett.* **93**, 068701 (2004).
- [56] S. Meloni, J. G.-G. nes, V. Latora, and Y. Moreno, *Phys. Rev. Lett.* **100**, 208701 (2008).
- [57] Z. Eisler, I. Bartos, and J. Kertész, *Adv. Phys.* **57**, 89 (2008).
- [58] J. Nacher, T. Ochiai, and T. Akutsu, *Mod. Phys. Lett. B* **19**, 1169 (2005).
- [59] A. Bar-Even, J. Paulsson, N. Maheshri, M. CArmi, E. O'Shea, Y. Pilpel, and N. Barkai, *Nat. Genet.* **38**, 636 (2006).
- [60] M. B. Elowitz, A. J. Levine, E. D. Siggia, and P. S. Swain, *Science* **297**, 1183 (2002).
- [61] P. S. Swain, M. B. Elowitz, and E. D. Siggia, *Proc. Nat'l. Acad. Sci. U.S.A.* **99**, 12795 (2002).